Check for updates

Research Article

INTERNATIONAL JOURNAL OF ADVANCED ROBOTIC SYSTEMS

International Journal of Advanced Robotic Systems
September-October 2016: 1–10
© The Author(s) 2016
DOI: 10.1177/1729881416657975
arx.sagepub.com
SAGE

Kinematics and dynamics analysis of a novel 2PC-CPR parallel mechanism

Sheng Lin[1], Shuilan Wang[1], Chun Wang[1], Lingxuan Zhang[2], and Yun Zhai[1]

Abstract

A novel parallel mechanism of two translations and one rotation freedom degrees two-prismatic joint-cylindrical joint-one-cylindrical joint-prismatic joint-revolute joint (2PC-CPR) is proposed. The mechanism can be applied to write Chinese characters and to classify productions with the appropriated control. In this article, the kinematics and dynamics analysis are systematically conducted with the following procedure. First of all, the 2PC-CPR parallel mechanism is designed by G_F set and the freedom degree of the mechanism is calculated using screw theory. Then the formula for solving the inverse/forward displacement, velocity, and acceleration is derived based on the geometrical constraints. The dynamics model is established by using virtual work principle. Finally, kinematics SimMechanics model is created by the co-simulation of SolidWorks and MATLAB software, and its workspace is analyzed.

Keywords

Parallel mechanism, kinematics, dynamics, workspace

Date received: 11 February 2016; accepted: 21 May 2016

Topic: Robot Manipulation and Control
Topic Editor: Andrey V Savkin
Associate Editor: Bojan Nemec

Introduction

Parallel robots with three freedom degrees have the advantages such as simple structure, low cost, highly targeted. It has a broad application prospect in the fields of parallel robot. Some parallel mechanisms with three translation freedom degrees have drawn significant attention by researchers these years. Tsai[1] invented a parallel mechanism of three-universal hinge-prismatic joint-universal hinge(3-UPU), and it is studied by many scholars later.[2–6] Carricato and Parenti-Castelli[7,8] proposed and analyzed a series of isotropic three-translational parallel mechanisms. Kong[9] proposed a parallel mechanism of three-cylindrical joint-revolute joint-revolute joint (3-CRR), and its kinematics and singular problem were analyzed. Li[10] researched a novel parallel mechanism of three-prismatic joint-revolute joint and cylindrical joint (3-PRC) with over constraints. Ruggiu[11] presented a translational parallel mechanism of three-cylindrical joint-universal hinge-revolute joint (3-CUR) and analyzed its kinematics. Kim[12] proposed the sufficient and necessary conditions of constituting a three-translational parallel mechanism. Some parallel mechanisms with three rotation freedom degrees were also investigated. Gosselin[13] proposed a type of parallel mechanism with three rotation freedom degrees, and its singular pose was analyzed. Karouia and Hervé[14] proposed a kind of pure rotation 3-UPU parallel mechanism and Di Gregorio[15] researched its singular and static problems. Besides, Huang[16] integrated some different 3-UPU parallel mechanism and analyzed their kinematics characteristics. Lu and Hu[17] constructed a type of parallel mechanisms of two-universal hinge-prismatic joint-universal hinge plus X joint (2UPU+X). Research of the mechanism with three freedom degrees is mainly focused on the symmetric mechanism with pure rotation or pure translation. The type of asymmetric parallel mechanisms with one

[1] School of Mechanical Engineering, Dalian Jiaotong University, Dalian, China
[2] Key laboratory of space Structure and Mechanism Technology, Shanghai, China

Corresponding author:
Shuilan Wang, School of Mechanical Engineering, Dalian Jiaotong University, Dalian 116028, China.
Email: wslan_123@163.com

Creative Commons CC-BY: This article is distributed under the terms of the Creative Commons Attribution 3.0 License (http://www.creativecommons.org/licenses/by/3.0/) which permits any use, reproduction and distribution of the work without further permission provided the original work is attributed as specified on the SAGE and Open Access pages (https://us.sagepub.com/en-us/nam/open-access-at-sage).

Table 1. Classification of G_F sets.

Dimension	Translation	Rotation	Type	The G_F sets
6	3	3	3T3R	$G_F^{3T3R} = (T_a \quad T_b \quad T_c; \quad R_a \quad R_\beta \quad R_\gamma)$
5	3	2	3T2R	$G_F^{3T2R} = (T_a \quad T_b \quad T_c; \quad R_a \quad R_\beta \quad 0)$
	2	3	2T3R	$G_F^{2T3R} = (T_a \quad T_b \quad 0; \quad R_a \quad R_\beta \quad R_\gamma)$
	3	1	3T1R	$G_F^{3T1R} = (T_a \quad T_b \quad T_c; \quad R_a \quad 0 \quad 0)$
4	2	2	2T2R	$G_F^{2T2R} = (T_a \quad T_b \quad 0; \quad R_a \quad R_\beta \quad 0)$
	1	3	1T3R	$G_F^{1T3R} = (T_a \quad 0 \quad 0; \quad R_a \quad R_\beta \quad R_\gamma)$
	3	0	3T	$G_F^{3T} = (T_a \quad T_b \quad T_c; \quad 0 \quad 0 \quad 0)$
3	2	1	2T1R	$G_F^{2T1R} = (T_a \quad T_b \quad 0; \quad R_a \quad 0 \quad 0)$
	1	2	1T2R	$G_F^{1T2R} = (T_a \quad 0 \quad 0; \quad R_a \quad R_\beta \quad 0)$
	0	3	3R	$G_F^{3R} = (0 \quad 0 \quad 0; \quad R_a \quad R_\beta \quad R_\gamma)$
	2	0	2T	$G_F^{2T} = (T_a \quad T_b \quad 0; \quad 0 \quad 0 \quad 0)$
2	1	1	1T1R	$G_F^{1T1R} = (T_a \quad 0 \quad 0; \quad R_a \quad 0 \quad 0)$
	0	2	2R	$G_F^{2R} = (0 \quad 0 \quad 0; \quad R_a \quad R_\beta \quad 0)$
1	1	0	1T	$G_F^{1T} = (T_a \quad 0 \quad 0; \quad 0 \quad 0 \quad 0)$
	0	1	1R	$G_F^{1R} = (0 \quad 0 \quad 0; \quad R_a \quad 0 \quad 0)$
0	0	0	0	$G_F^{0} = (0 \quad 0 \quad 0; \quad 0 \quad 0 \quad 0)$

translation and two rotations or two translations and one rotation has been in the lack of investigation. However, the requirement for novel asymmetric parallel mechanism with three freedom degrees will gradually increase with the application of the robot in various fields.

To meet the increasing need in the robot field, a novel 2PC-CPR parallel mechanism is proposed and the following works are done in this article.

(1) A novel 2PC-CPR parallel mechanism with two translations and one rotation is designed using G_F set. The mechanism can be applied to write Chinese characters and classify products.
(2) The freedom degree of the mechanism is calculated with screw theory.
(3) The formula for solving the inverse/forward displacement kinematics, velocity, and acceleration is derived. The dynamics model is established.
(4) The SimMechanics model of kinematics is created by the co-simulation of SolidWorks and MATLAB to verify the correctness of theoretical derivations. The workspace is analyzed.

Design of 2T1R parallel mechanism and its freedom degrees

The establishment of 2T1R parallel mechanism

To obtain a two translations and one rotation (2T1R) parallel mechanism, G_F set is selected as the method to synthesize the mechanism. G_F set is used to describe the motion features of the robot mechanism end. All the freedom degrees of the robot mechanism end include three translations and three rotations. Then the mechanism end definition in G_F sets can be expressed as follows[18,19]

$$G_F = (T_a \quad T_b \quad T_c; \quad R_\alpha \quad R_\beta \quad R_\gamma) \tag{1}$$

where T_a, T_b, and T_c denote three translations of the mechanism end, subscript a, b, and c denote three noncoplanar movement direction vectors; R_α, R_β, and R_γ denote the three rotations of the mechanism end; subscript α, β, and γ denote three noncoplanar rotation direction vectors.

The motion characteristics of the robot mechanism can be qualitatively described by each item of the G_F set. G_F set can be classified into seven categories according to the number of the dimension, which is shown in Table 1.

As the configuration synthesis of G_F set, we can obtain the novel 2PC-CPR parallel mechanism with the following steps.

Step 1: Design a three-degree freedom parallel mechanism with 2T1R, the motion feature can be described by G_F set as: $G_F = (T_a \; T_b \; 0; \; R_a \; 0 \; 0)$.Where T_a represents the translation along the direction of a, T_b represents the translation along the direction of b, and R_α represents the rotation around the direction α.
Step 2: Determine the number of kinematic branch. For the input number of the mechanism is equal to number of the degree of freedom, the mechanism has three kinematic branches.
Step 3: Determine the type of kinematic branches as two 2T1R branches and a 3T1R branch. Then the three branches are denoted as: $G_{F1} = (T_{a1} \; T_{b1} \; 0; \; R_{a1} \; 0 \; 0)$, $G_{F2} = (T_{a2} \; T_{b2} \; 0; \; R_{a2} \; 0 \; 0)$, and $G_{F3} = (T_{a3} \; T_{b3} \; T_{c3}; \; R_{a3} \; 0 \; 0)$ in G_F set. Then we can obtain the mechanism with three freedom degrees by intersection rule $G_F = G_{F1} \cap G_{F2} \cap G_{F3} = (T_a \; T_b \; 0; \; R_a \; 0 \; 0)$. The intersection of three kinematic branches is shown in Figure 1.
Step 4: Determine the kinematic pairs on kinematic branches. The first and the second kinematic branches can be made of a sliding pair and a cylindrical pair, and the third kinematic branch can be made of a cylindrical pair, a sliding pair, and a revolute pair.

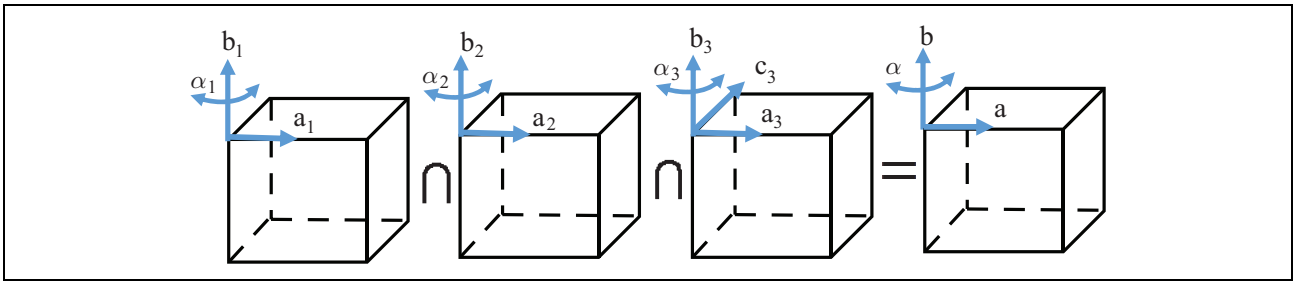


Figure 1. The intersection of three kinematic chains.

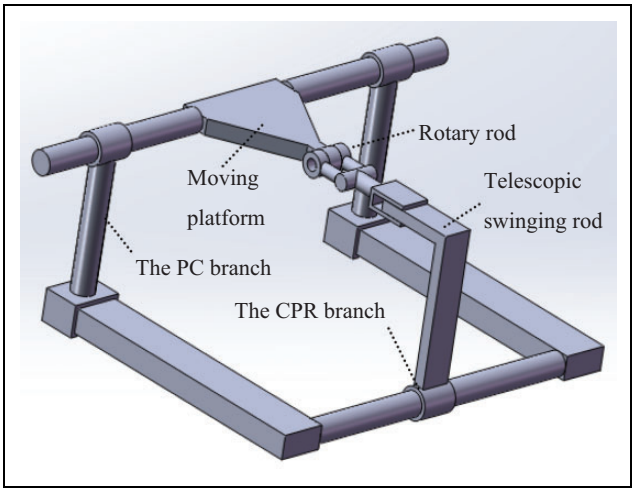


Figure 2. The three-dimensional model of 2PC-CPR parallel mechanism.

Step 5: Determine the spatial position relationship. The translation plane of the two 2T1R kinematic branches is parallel and the rotation axis is coincident; the rotation axis of 2T1R kinematic branch is parallel with the rotation axis of 3T1R kinematic branch. Then the three-dimensional model is constructed in Figure 2.

The DOF of 2PC-CPR parallel mechanism

According to the modified Grübler–Kutzbach criterion,[20] the degree of freedom can be calculated by the equation as follows

$$M = d(n - g - 1) + \sum_{i}^{g} f_i + v \tag{2}$$

where d is the order of a mechanism and related to common constraint, n is the number of components include the frame, g is the number of kinematic pair, f_i is the degree of freedom of the i kinematic pair, and v is the redundant constraint for parallel mechanism.

Screw theory is introduced to describe the constraints in single kinematic branch, and then all branch constraints are synthesized to calculate the corresponding degrees of freedom according to equation (2). A screw can be

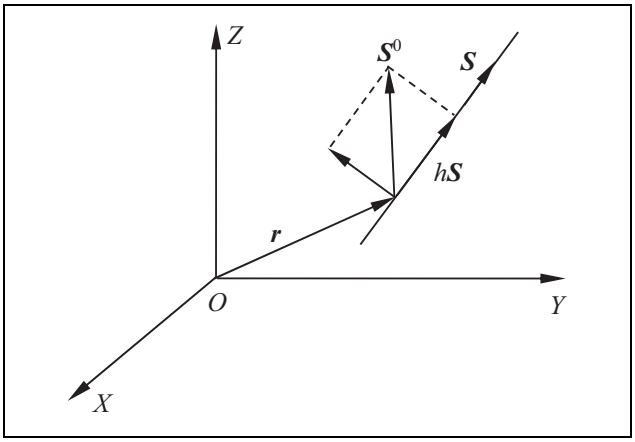


Figure 3. The components of a screw.

expressed as equation (3). All the components of a screw is shown in Figure 3

$$\$ = (\boldsymbol{S}; \boldsymbol{S}^0) = (\boldsymbol{S}; \boldsymbol{S}_0 + h\boldsymbol{S}) \tag{3}$$

where $\boldsymbol{S}$ is the unit vector, $\boldsymbol{S}_0 = \boldsymbol{r} \times \boldsymbol{S}$ is the moment of the unit vector $\boldsymbol{S}$ about the origin O, and h is the pitch.

According to the value of h, two types of special screw can be expressed as

$$\begin{cases} \$ = (\boldsymbol{S}; \boldsymbol{S}_0) \ (h = 0) \\ \$ = (\boldsymbol{0}; \boldsymbol{S}) \ (h = \infty) \end{cases} \tag{4}$$

Two screws are denoted as $\$_1 = (\boldsymbol{S}_1; \boldsymbol{S}_1^0)$ and $\$_2 = (\boldsymbol{S}_2; \boldsymbol{S}_2^0)$, then the reciprocal product of two screws is defined as[21]

$$\$_1 \circ \$_2 = \boldsymbol{S}_1 \cdot \boldsymbol{S}_2^0 + \boldsymbol{S}_2 \cdot \boldsymbol{S}_1^0 \tag{5}$$

where the symbol $\circ$ denotes the reciprocal product of two screws.

If the reciprocal product is $\$ \circ \$^r = 0$, $\$^r$ is called the reciprocal screw of $\$$. For a motion screw system, a reciprocal screw system constrains the motions of the body while some remaining freedoms are retained. Then the motion screw and reciprocal screw can be denoted as

$$\begin{aligned} \$ &= (w_x \quad w_y \quad w_z; \quad v_x \quad v_y \quad v_z) \\ \$^r &= (F_x \quad F_y \quad F_z; \quad M_x \quad M_y \quad M_z) \end{aligned} \tag{6}$$

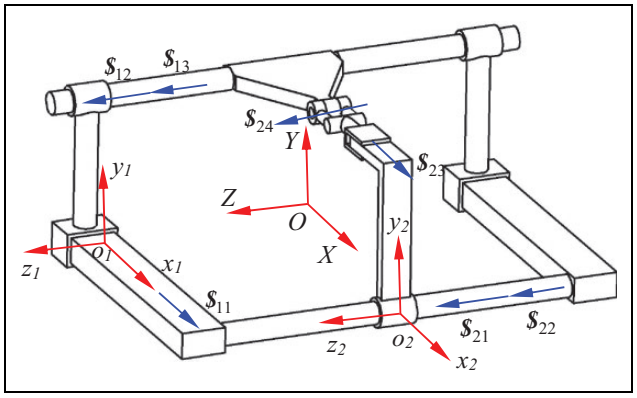


Figure 4. The kinematic screws of PC and CPR branches.

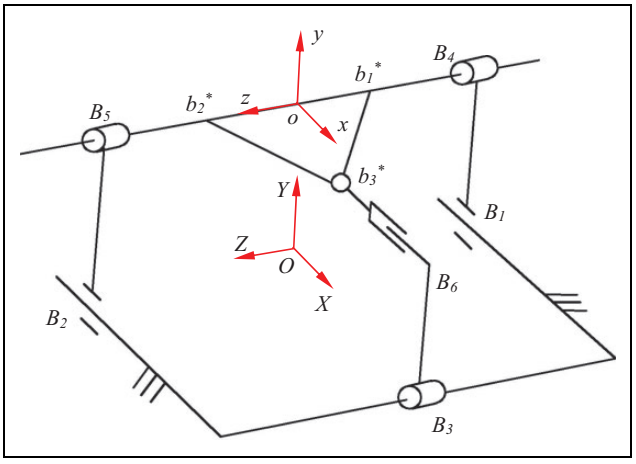


Figure 5. The hinge coordinates of the 2PC-CPR parallel mechanism.

where $w_i(i = x, y \text{ and } z)$ is the angular velocity around x, y, and z axis; $v_i(i = x, y \text{ and } z)$ is the velocity along x, y, and z axis; $F_i(i = x, y \text{ and } z)$ is the force constraints along x, y, and z axis; and $M_i(i = x, y \text{ and } z)$ is the moment constraints around x, y, and z axis.

To obtain the common constraints in equation (2), two local coordinate systems $o_1x_1y_1z_1$ and $o_2x_2y_2z_2$ are established on two kinematic branches, respectively. The global coordinate system $OXYZ$ is established on the base. All the kinematic screws of the PC and CPR branches are shown in Figure 4. In the first kinematic branch, the sliding pair is denoted by the kinematic screw $\$_{11}$. And the cylindrical pair is denoted by the two screws $\$_{12}$ and $\$_{13}$. According to equation (4), the screw system of the first kinematic branch is expressed as follows

$$\begin{aligned} \$_{11} &= (0 \quad 0 \quad 0; \quad 1 \quad 0 \quad 0) \\ \$_{12} &= (0 \quad 0 \quad 0; \quad 0 \quad 0 \quad 1) \\ \$_{13} &= (0 \quad 0 \quad 1; \quad 0 \quad 0 \quad 0) \end{aligned} \tag{7}$$

The constraint screw system is the reciprocal screws of equation (7). According to equations (5) and (6), the constraint screws are as follows

$$\begin{aligned} \$_{11}{}^r &= (0 \quad 1 \quad 0; \quad 0 \quad 0 \quad 0) \\ \$_{12}{}^r &= (0 \quad 0 \quad 0; \quad 1 \quad 0 \quad 0) \\ \$_{13}{}^r &= (0 \quad 0 \quad 0; \quad 0 \quad 1 \quad 0) \end{aligned} \tag{8}$$

The constraint screw system includes a force line vector and two moments. The translation along y-axis is constrained by the force, and the rotations around x-axis and y-axis are constrained by the two moments.

Similarly, the screw system of the second kinematic branch is as follows

$$\begin{aligned} \$_{21} &= (0 \quad 0 \quad 0; \quad 0 \quad 0 \quad 1) \\ \$_{22} &= (0 \quad 0 \quad 1; \quad 0 \quad 0 \quad 0) \\ \$_{23} &= (0 \quad 0 \quad 0; \quad a_1 \quad b_1 \quad 0) \\ \$_{23} &= (0 \quad 0 \quad 1; \quad a_2 \quad b_2 \quad 0) \end{aligned} \tag{9}$$

The kinematic screw system is composed of four independent screws, then the constraint screws are as follows

$$\begin{aligned} \$_{21}{}^r &= (0 \quad 0 \quad 0; \quad 1 \quad 0 \quad 0) \\ \$_{22}{}^r &= (0 \quad 0 \quad 0; \quad 0 \quad 1 \quad 0) \end{aligned} \tag{10}$$

The constraint screw system includes two moments, which constrains the rotations around x-axis and y-axis.

Then the mechanism has two common constraints and zero redundant constraint. The degree of freedom can be obtained according to equation (2)

$$M = (6 - 2)(5 - 5 - 1) + 7 = 3 \tag{11}$$

Therefore, the freedom degree of the mechanism is 3, which are translations along the x-axis and z-axis, and rotations around z-axis.

Table 2. The structure parameter coordinates.

Hinge point	Coordinate	Hinge point	Coordinate
$b_1{}^*$	(0, 0, $-a$)	B_1	(0, 0, $-3a$)
$b_2{}^*$	(0, 0, a)	B_2	(0, 0, $3a$)
$b_3{}^*$	($2a$, 0, 0)	B_3	($5a$, 0, 0)
B_4	(0, h,$-3a$)	B_6	($5a$, h, 0)

The kinematic analysis

Inverse solution for displacement

The coordinate system $oxyz$ is established on the upper platform in Figure 5. The vector coordinates of structure parameters is shown in Table 2.

The terminal position and orientation of the moving platform is denoted as $(x, y, z, \alpha, \beta, \gamma)$. The freedom degrees of the mechanism are translations along x-axis and z-axis and rotation around z-axis, so the following equations are obtained as

$$\left.\begin{aligned} y &= h \\ \alpha &= \beta = 0 \end{aligned}\right\} \tag{12}$$

Table 3. The hinge point coordinates.

Hinge point	Coordinate	Hinge point	Coordinate
B_1	$(z_1, 0, -3a)$	B_4	$(z_1, h, -3a)$
B_2	$(z_1, 0, 3a)$	B_5	$(z_1, h, 3a)$
B_3	$(5a, 0, z_2)$	B_6	$(5a + hs\varphi, hc\varphi, z_2)$

The coordinate of the hinge point in the moving coordinate system is denoted as $(b_1^*, b_2^*, b_3^*)^T$, and the coordinate of the hinge point in the fixed coordinate system is set as $(b_1, b_2, b_3)^T$. Then the relationship between $(b_1^*, b_2^*, b_3^*)^T$ and $(b_1, b_2, b_3)^T$ can be expressed as

$$\begin{bmatrix} b_1 \\ b_2 \\ b_3 \end{bmatrix} = \mathbf{R} \begin{bmatrix} b_1^* \\ b_2^* \\ b_3^* \end{bmatrix} + [x \quad h \quad z]^T \tag{13}$$

where $\mathbf{R} = \begin{bmatrix} c_\gamma & -s_\gamma & 0 \\ s_\gamma & c_\gamma & 0 \\ 0 & 0 & 1 \end{bmatrix}$ is the direction cosine matrix of the moving platform in the fixed coordinate system. Then the coordinate in the fixed system is as follows

$$\begin{aligned} \begin{bmatrix} b_1 \\ b_2 \\ b_3 \end{bmatrix} &= \begin{bmatrix} c_\gamma & -s_\gamma & 0 \\ s_\gamma & c_\gamma & 0 \\ 0 & 0 & 1 \end{bmatrix} \begin{bmatrix} 0 & 0 & 2a \\ 0 & 0 & 0 \\ -a & a & 0 \end{bmatrix} + [x \quad h \quad z]^T \\ &= \begin{bmatrix} x & x & x + 2ac_\gamma \\ h & h & h + 2as_\gamma \\ z - a & z + a & z \end{bmatrix} \end{aligned} \tag{14}$$

The displacement of the sliding pair in the first branch is denoted as z_1 along the x-axis, and the displacement of the cylindrical pair in the second branch is denoted as z_2 along the z-axis. The rotation angle of cylindrical pair in second branch is denoted as φ around z-axis. Then the hinge point coordinates are expressed as Table 3. According to the geometric constraints, equation (15) is obtained

$$\left.\begin{aligned} \overline{b_1B_1}^2 &= h^2 + (2a + z_2)^2 \\ \overline{b_2B_2}^2 &= h^2 + (2a - z_2)^2 \\ \overline{b_3B_3}^2 - \overline{b_3B_6}^2 &= h^2 \end{aligned}\right\} \tag{15}$$

Substituting the hinge point coordinates into equation (15), equation (16) is derived as follows

$$\left.\begin{aligned} &(x - z_1)^2 + h^2 + (z + 2a)^2 = h^2 + (2a + z_2)^2 \\ &(x - z_1)^2 + h^2 + (z - 2a)^2 = h^2 + (2a - z_2)^2 \\ &(x + 2ac_\gamma - 5a)^2 + (h + 2as_\gamma)^2 + (z - z_2)^2 \\ &-(x + 2ac_\gamma - 5a - hs_\varphi)^2 - (h + 2as_\gamma - hc_\varphi)^2 - (z - z_2)^2 = h^2 \end{aligned}\right\} \tag{16}$$

Then the inverse solution equation of displacement can be obtained as follows

$$\left.\begin{aligned} z_1 &= x \\ z_2 &= z \\ \varphi &= \arcsin(h \bullet \sqrt{A^2 + B^2}) - M \end{aligned}\right\} \tag{17}$$

where $A = h + 2as_\gamma$, $B = x + 2ac_\gamma - 5a$, and $M = \frac{A}{B}$.

Forward solution for displacement

In the forward solution of displacement, x, z, and γ should be obtained according to z_1, z_2, and φ. From equation (17), we can obtain the forward solution equation of displacement as follows

$$\left.\begin{aligned} x &= z_1 \\ z &= z_2 \\ \gamma &= \varphi - \arcsin\frac{h + (5a + z_1)s_\varphi - hc_\varphi}{2a} \end{aligned}\right\} \tag{18}$$

Inverse velocity analysis

The relationship between input and output displacement is given in equation (18). By differentiation of equation (18) with respect to time, the relationship between the input speed and output velocity is derived as follows

$$\left.\begin{aligned} &\dot{x} = \dot{z}_1 \\ &\dot{z} = \dot{z}_2 \\ &-s_\varphi \dot{x} + 2a(s_\gamma s_\varphi - c_\gamma c_\varphi)\dot{\gamma} = [(2ac_\gamma + x - 5a)c_\varphi - (2as_\gamma + h)s_\varphi]\dot{\varphi} \end{aligned}\right\} \tag{19}$$

Matrix form of equation (19) can be expressed as

$$[\dot{z}_1 \quad \dot{z}_2 \quad \dot{\varphi}]^T = \boldsymbol{J}_m [\dot{x} \quad \dot{z} \quad \dot{\gamma}]^T \tag{20}$$

where $\boldsymbol{J}_m = \begin{bmatrix} 1 & 0 & 0 \\ 0 & 1 & 0 \\ \frac{-s_\varphi}{(2ac_\gamma + x - 5a)c_\varphi - (2as_\gamma + h)s_\varphi} & 0 & \frac{2a(s_\gamma s_\varphi + c_\gamma c_\varphi)}{(2ac_\gamma + x - 5a)c_\varphi - (2as_\gamma + h)s_\varphi} \end{bmatrix}$.

Forward velocity analysis and Jacobian matrix

equation (19) can also be written as follows

$$\boldsymbol{J}_x [\dot{x} \quad \dot{z} \quad \dot{\gamma}]^T = \boldsymbol{J}_q [\dot{z}_1 \quad \dot{z}_2 \quad \dot{\varphi}]^T \tag{21}$$

where $\boldsymbol{J}_\mathbf{x} = \begin{bmatrix} 1 & 0 & 0 \\ 0 & 1 & 0 \\ -s_\varphi & 0 & 2a(s_\gamma s_\varphi - c_\gamma c_\varphi) \end{bmatrix}$ and $\boldsymbol{J_q} = \begin{bmatrix} 1 & 0 & 0 \\ 0 & 1 & 0 \\ 0 & 0 & (2ac_\gamma + x - 5a)c_\varphi - (2as_\gamma + h)s_\varphi \end{bmatrix}$.

If $2a(s_\gamma s\varphi - c_\gamma c\varphi) \neq 0, |\boldsymbol{J}_x| \neq 0$, forward velocity analysis are derived as follows

$$[\dot{x} \quad \dot{z} \quad \dot{\gamma}]^T = \boldsymbol{J}_\alpha [\dot{z}1 \quad \dot{z}2 \quad \dot{\varphi}]^T \tag{22}$$

where $\boldsymbol{J}_\alpha = \boldsymbol{J}_x^{-1} \boldsymbol{J}_q$.

Then the Jacobian matrix $\boldsymbol{J}_\alpha$ can be obtained as

$$\boldsymbol{J}_\alpha = \boldsymbol{J}_x^{-1}\boldsymbol{J}_q = \begin{bmatrix} 1 & 0 & 0 \\ 0 & 1 & 0 \\ \dfrac{s_\varphi}{2a(s_\gamma s_\varphi - c_\gamma c_\varphi)} & 0 & \dfrac{(2ac_\gamma + x - 5a)c_\varphi - (2as_\gamma + h)s_\varphi}{2a(s_\gamma s_\varphi - c_\gamma c_\varphi)} \end{bmatrix} \tag{23}$$

Acceleration analysis

By differentiation of equation (19) with respect to time, the relationship between the input and output acceleration is derived as

$$\left.\begin{array}{l} \ddot{z}_1 = \ddot{x} \\ \ddot{z}_2 = \ddot{z} \\ \left(-s_\varphi \dot{x} + 2a(\dot{s}_\gamma s_\varphi - c_\gamma c_\varphi)\dot{\gamma}\right) = \left((2ac_\gamma + x - 5a)c_\varphi\ \dot{\varphi} - (2as_\gamma + h)s_\varphi\ \dot{\varphi}\right) \end{array}\right\} \tag{24}$$

Matrix form of equation (24) can be written as

$$\ddot{\varphi} = \begin{bmatrix} \dot{x} & \dot{\gamma} \end{bmatrix}\begin{bmatrix} H_{11} & H_{12} \\ H_{21} & H_{22} \end{bmatrix}\begin{bmatrix} \dot{x} \\ \dot{\gamma} \end{bmatrix} + \begin{bmatrix} G_1 & G_2 \end{bmatrix}\begin{bmatrix} \ddot{x} \\ \ddot{\gamma} \end{bmatrix} \tag{25}$$

where $H_{11} = -2G_1G_4 + {G_1}^2G_3$, $H_{12} = H_{21} = -G_2G_4 + G_1G_5 + G_1G_2G_3$, $H_{22} = 2G_2G_5 + G_5 + {G_2}^2G_3$, $G_1 = \frac{-s_\varphi}{(2ac_\gamma + x - 5a)c_\varphi - (2as_\gamma + h)s_\varphi}$, $G_2 = \frac{2a(s_\gamma s_\varphi - c_\gamma c_\varphi)}{(2ac_\gamma + x - 5a)c_\varphi - (2as_\gamma + h)s_\varphi}$, $G_3 = \frac{(2ac_\gamma + x - 5a)s_\varphi + (2as_\gamma + h)c_\varphi}{(2ac_\gamma + x - 5a)c_\varphi - (2as_\gamma + h)s_\varphi}$, $G_4 = \frac{c_\varphi}{(2ac_\gamma + x - 5a)c_\varphi - (2as_\gamma + h)s_\varphi}$, and $G_5 = \frac{2a(s_\gamma c_\varphi + c_\gamma s_\varphi)}{(2as_\gamma - h)s_\varphi + (2ac_\gamma + x - 5a)c_\varphi}$.

The dynamics model

According to the virtual work principle,[22,23] the sum of the virtual work generated by the arbitrary virtual displacement is zero. Then virtual work generated by the joint space virtual displacement is equal to the virtual work generated by the virtual displacement of operating space. It can be expressed as equation (26)

$$\tau^T \bullet \delta \boldsymbol{q} = \boldsymbol{F}^T \bullet \boldsymbol{D} \tag{26}$$

where τ is the force or torque vector of each joint, $\delta \boldsymbol{q}$ is the virtual displacement of each joint, $\boldsymbol{F}$ is the generalized force vector on the center of the moving platform, and $\boldsymbol{D}$ is the virtual displacement of the moving platform center.

The relationship of the virtual displacements $\boldsymbol{D}$ and $\delta \boldsymbol{q}$ is determined by the Jacobian matrix as follows

$$\boldsymbol{D} = \boldsymbol{J}\,\delta\,\boldsymbol{q} \tag{27}$$

Substitute equation (27) into equation (26), we can obtain the equation (28)

$$\tau = \boldsymbol{J}^{\mathrm{T}}\boldsymbol{F} \tag{28}$$

The establishment of dynamic model

For the parallel mechanism, the driving force from the PC and CPR drive branch should be balanced with the equivalent driving force transformed from moving platform. Then the dynamic model is established as follows

$$\tau + \boldsymbol{F}_{Eo} + \sum_{i=1}^{2} \boldsymbol{F}_{Emi} + \boldsymbol{F}_{ED} = 0 \tag{29}$$

where $\tau = (\boldsymbol{f}_1 \quad \boldsymbol{f}_2 \quad \boldsymbol{f}_3)^T$ is the driving force of three branch drivers, $\boldsymbol{F}_{Eo}$ is the equivalent driving force of moving platform, $\boldsymbol{F}_{Emi}$ is equivalent driving force of the PC branch, and $\boldsymbol{F}_{ED}$ is equivalent driving force of the CPR branch.

The influence of friction is not considered, and the bar mass center is simplified to the geometric center. Combining equation (28) and equation (29), the equivalent driving force can be expressed as follows

$$\left.\begin{array}{r} \boldsymbol{F}_{Eo} = (\boldsymbol{J}_\alpha)^T\begin{bmatrix} \boldsymbol{f}_{co} + \boldsymbol{G}_{co} + \boldsymbol{F}_{co} \\ \boldsymbol{n}_{co} + \boldsymbol{M}_{co} \end{bmatrix} \\ \boldsymbol{F}_{Emi} = (\boldsymbol{J}_m)^T\begin{bmatrix} \boldsymbol{f}_{cmi} + \boldsymbol{G}_{cmi} \\ \boldsymbol{n}_{cmi} \end{bmatrix} \\ \boldsymbol{F}_{ED} = (\boldsymbol{J}_u)^T\begin{bmatrix} \boldsymbol{f}_{cu} + \boldsymbol{G}_{cu} \\ \boldsymbol{n}_{cu} \end{bmatrix} + (\boldsymbol{J}_s)^T\begin{bmatrix} \boldsymbol{f}_{cs} + \boldsymbol{G}_{cs} \\ \boldsymbol{n}_{cs} \end{bmatrix} \end{array}\right\} \tag{30}$$

where $\boldsymbol{J}_\alpha$ is the Jacobian matrix,$\boldsymbol{f}_{co}$ is the inertial force, $\boldsymbol{n}_{co}$ is the inertia torque, $\boldsymbol{G}_{co}$ is the gravitation, $\boldsymbol{F}_{co}$ is the external force, and $\boldsymbol{M}_{co}$ is the external torque of the moving platform. $\boldsymbol{J}_m$ is the Jacobian matrix,$\boldsymbol{f}_{cmi}$ is the inertial force, $\boldsymbol{G}_{cmi}$ is the gravitation, and $\boldsymbol{n}_{cmi}$ is the inertia torque of the PC branch. $\boldsymbol{J}_u$ is the Jacobian matrix,$\boldsymbol{f}_{cu}$ is the inertial force, $\boldsymbol{G}_{cu}$ is the gravitation, and $\boldsymbol{n}_{cu}$ is the inertia torque of telescopic swinging rod. $\boldsymbol{J}_s$ is the Jacobian matrix, $\boldsymbol{f}_{cs}$ is the inertial force, $\boldsymbol{G}_{cs}$ is the gravitation, and $\boldsymbol{n}_{cs}$ is the inertia torque of rotary rod.

The calculation of the force and torque

According to Newton's second law and Lagrangian equation, the parameters $\boldsymbol{f}_{co}$, $\boldsymbol{n}_{co}$, $\boldsymbol{G}_{co}$, $\boldsymbol{f}_{cmi}$, $\boldsymbol{n}_{cmi}$, $\boldsymbol{G}_{cmi}$, $\boldsymbol{f}_{cu}$, $\boldsymbol{n}_{cu}$, $\boldsymbol{G}_{cs}$, $\boldsymbol{f}_{cs}$, $\boldsymbol{n}_{cs}$, and $\boldsymbol{G}_{cu}$ in equation (30) can be calculated by the following

$$\left.\begin{array}{c} \boldsymbol{f}_{co} = -m_o\dot{\boldsymbol{v}}_{co} \\ \boldsymbol{n}_{co} = -\boldsymbol{I}_{co}\dot{\boldsymbol{w}}_{co} - \boldsymbol{w}_{co} \times (\boldsymbol{I}_{co}\boldsymbol{w}_{co}) \\ \boldsymbol{G}_{co} = m_o\boldsymbol{g} \\ \boldsymbol{f}_{cmi} = -m_m\dot{\boldsymbol{v}}_{cmi} \\ \boldsymbol{n}_{cmi} = -\boldsymbol{I}_{cmi}\dot{\boldsymbol{w}}_{cmi} - \boldsymbol{w}_{cmi} \times (\boldsymbol{I}_{cmi}\boldsymbol{w}_{cmi}) \\ \boldsymbol{G}_{co} = m_m\boldsymbol{g} \\ \boldsymbol{f}_{cu} = -m_u\dot{\boldsymbol{v}}_{cu} \\ \boldsymbol{n}_{cu} = -\boldsymbol{I}_{cu}\dot{\boldsymbol{w}}_{cu} - \boldsymbol{w}_{cu} \times (\boldsymbol{I}_{cu}\boldsymbol{w}_{cu}) \\ \boldsymbol{G}_{cu} = m_u\boldsymbol{g} \\ \boldsymbol{f}_{cs} = -m_s\dot{\boldsymbol{v}}_{cs} \\ \boldsymbol{n}_{cs} = -\boldsymbol{I}_{cs}\dot{\boldsymbol{w}}_{cs} - \boldsymbol{w}_{cs} \times (\boldsymbol{I}_{cs}\boldsymbol{w}_{cs}) \\ \boldsymbol{G}_{cs} = m_s\boldsymbol{g} \end{array}\right\} \tag{31}$$

where m_o and $\boldsymbol{I}_{co}$ are the mass and inertia of moving platform, m_m and $\boldsymbol{I}_{cmi}$ are the mass and inertia of PC branch, m_{cu} and $\boldsymbol{I}_{cu}$ are the mass and inertia of telescopic swinging, and m_{cs} and $\boldsymbol{I}_{cs}$ are the mass and inertia of rotary rod.

The calculation of Jacobian matrix

(1) Jacobian matrix between moving platform and drive components

Suppose that the point o is the mass center of moving platform, then the velocity relationship between point o and drive components is obtained by equation (22). And then the Jacobian matrix between moving platform and drive components is $\boldsymbol{J}_\alpha$ in equation (23).

(2) Jacobian matrix between the PC branch and drive components

In the fixed coordinate system, the velocity of PC branch mass center is set as $[\mathbf{v}_{cmi}, \mathbf{w}_{cmi}]^T$. Then the relationship with drive components can be expressed as follows

$$[\mathbf{v}_{cmi} \quad \boldsymbol{w}_{cmi}]^T = \boldsymbol{J}_{mi}[\dot{z}_1 \quad \dot{z}_2 \quad \dot{\varphi}]^T, \ (i = 1, \ 2) \tag{32}$$

The mass center of PC component is on B_2B_5, and the centroid coordinates is denoted as(0, m, $3a$). Then the position and orientation of PC component mass center can be expressed as follows

$$x_{c1} = z_1, y_{c1} = m, z_{c1} = 3a, \alpha_{c1} = 0, \beta_{c1} = 0, \gamma_{c1} = 0 \tag{33}$$

By differentiation of equation (33) with respect to time, the Jacobian matrix $\boldsymbol{J}_{mi}$ can be obtained as

$$\boldsymbol{J}_{mi} = \begin{bmatrix} 1 & 0 & 0 \\ 0 & 0 & 0 \\ 0 & 0 & 0 \\ 0 & 0 & 0 \\ 0 & 0 & 0 \\ 0 & 0 & 0 \end{bmatrix} \tag{34}$$

(3) Jacobian matrix between the CPR branch and drive components

The driver branch is divided into telescopic swinging rod and rotary rod. In the fixed coordinate system, the mass center velocity of telescopic swinging rod is set as $[\mathbf{v}_{cs} \ \mathbf{w}_{cs}]^T$, and the mass center velocity of rotary rod is set as $[\mathbf{v}_{cu} \ \mathbf{w}_{cu}]^T$. The relationship between drive components can be expressed as

$$\left.\begin{array}{l} [\mathbf{v}_{cs} \quad \mathbf{w}_{cs}]^T = \boldsymbol{J}_s[\dot{z}_1 \quad \dot{z}_2 \quad \dot{\varphi}]^T \\ [\mathbf{v}_{cu} \quad \mathbf{w}_{cu}]^T = \boldsymbol{J}_u[\dot{z}_1 \quad \dot{z}_2 \quad \dot{\varphi}]^T \end{array}\right\} \tag{35}$$

The mass center of telescopic swinging rod is on B_3B_6, and the centroid coordinates is denoted as($5a$, n, 0). Then the position and orientation of telescopic swinging rod mass center can be expressed as follows

$$x_{cs} = 5a + ns_\varphi, y_{cs} = nc_\varphi, z_{cs} = z_2, \alpha_{cs} = 0, \beta_{cs} = 0, \gamma_{cs} = \varphi \tag{36}$$

By differentiation of equation (36) with respect to time, the Jacobian matrix $\boldsymbol{J}_s$ can be obtained as

$$\boldsymbol{J}_s = \begin{bmatrix} 0 & 0 & nc_\varphi \\ 0 & 0 & -ns_\varphi \\ 0 & 1 & 0 \\ 0 & 0 & 0 \\ 0 & 0 & 0 \\ 0 & 0 & 1 \end{bmatrix} \tag{37}$$

The mass center of rotary rod is on b_3B_6, and the distance between the centroid and b_3 is denoted as l. Then the position and orientation of rotary rod mass center can be expressed as follows

$$x_{cu} = z_1 + 2ac_\gamma + lc_\varphi, y_{cu} = h + 2as_\gamma - ls_\varphi, z_{cu} = z_2, \alpha_{cu} = 0, \beta_{cu} = 0, \gamma_{cu} = \varphi \tag{38}$$

By differentiation of equation (38) with respect to time, the Jacobian matrix $\boldsymbol{J}_u$ can be obtained as

$$\boldsymbol{J}_u = \begin{bmatrix} 1 - \frac{s_\gamma s_\varphi}{s_\gamma s_\varphi - c_\gamma c_\varphi} & 0 & -ls_\varphi + \frac{(2ac_\gamma + x - 5a)c_\varphi s_\gamma - (2as_\gamma + h)s_\varphi s_\gamma}{s_\gamma s_\varphi - c_\gamma c_\varphi} \\ \frac{c_\gamma s_\varphi}{s_\gamma s_\varphi - c_\gamma c_\varphi} & 0 & -lc_\varphi + \frac{(2ac_\gamma + x - 5a)c_\varphi c_\gamma - (2as_\gamma + h)s_\varphi c_\gamma}{s_\gamma s_\varphi - c_\gamma c_\varphi} \\ 0 & 1 & 0 \\ 0 & 0 & 0 \\ 0 & 0 & 0 \\ 0 & 0 & 1 \end{bmatrix} \tag{39}$$

where $\gamma = \varphi - \arcsin\dfrac{h + (5a + z_1)s_\varphi - hc_\varphi}{2a}$.

Then the driving force τ can be obtained if the external force $\boldsymbol{F}_{co}$ and the external torque $\mathbf{M}_{co}$ are given.

Kinematics simulation

Combining SolidWorks and MATLAB software, SimMechanics model is established in Figure 6. The physical environment parameters are set as kinematics. Three driver modules and a sensor measurement module are added to the SimMechanics model. Subsystem1, Subsystem2, and Subsystem3 in Figure 6 are package subsystems as Figure 7(a), (b), and (c), respectively.

For the parameters in Tables 2 and 3, a and h are set as 20 mm and 36 mm, respectively. z_1, φ and z_2 are changed according to ramp signal as Figure 8(a). The theory values of forward displacement solution in equation (18) can be expressed as the solid line in Figure 8(b). The position and posture of point o are obtained and shown as the dotted line in Figure 8(b). Therefore, the correctness of theoretical forward displacement solution of the parallel mechanism is verified.

Workspace analysis

In the kinematics SimMechanics model, the three ramp function inputs are changed. Then the workspace of mechanism can be acquired. Specific steps are as follows:

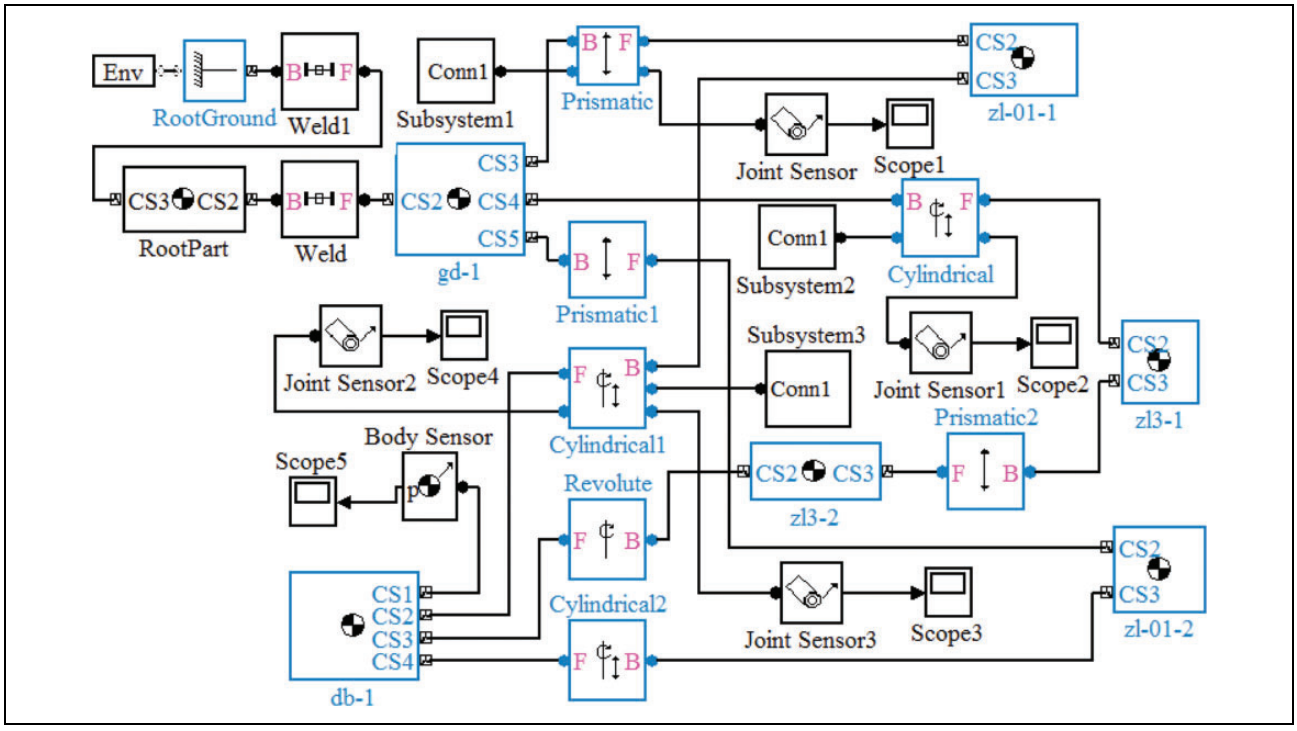


Figure 6. The kinematics model in SimMechanics. (a) Subsystem1, (b) Subsystem2, and (c) Subsystem3.

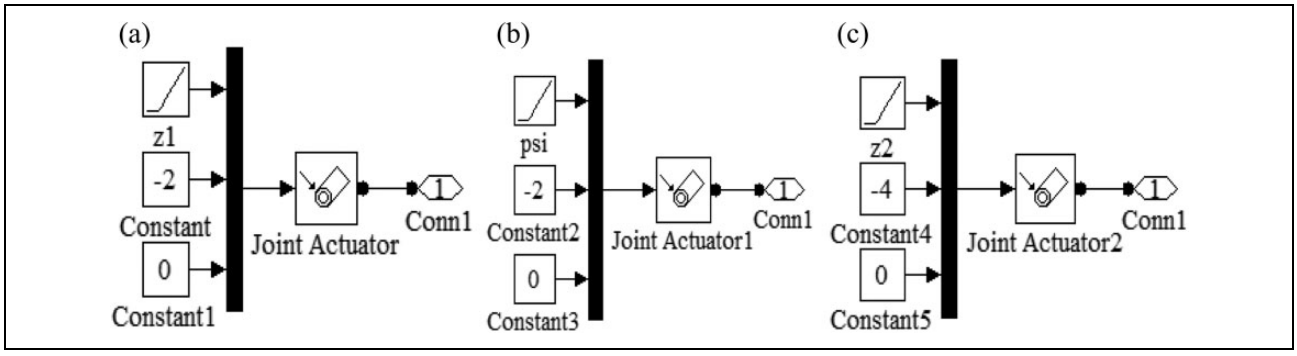


Figure 7. The package subsystems.

Step 1: Set the three input values range as $z_1 = (-15 \sim 10)$ m, $z_2 = (-20 \sim 20)$ m, $\varphi = (-20 \sim 10)$. The slope of the three inputs are $\delta_1 = 2.5$, $\delta_2 = 4$, $\delta_3 = 3$, and the number of growth is $n = 10$.

Step 2: Set $z_1 = -15 + i\delta_1$, $z_2 = -20 + (j-1)\delta_2 (j = 1, 2, \ldots, n+1)$, $\varphi = -20$.

Step 3: When $i = 0, 1, \ldots, n$, the data of step 2 are measured and saved.

Step 4: Set $z_1 = -15 + i\delta_1$, $z_2 = -20 + (j-1)\delta_2$ $(j = 1, 2, \ldots, n+1)$, $\varphi = 10$

Step 5: When $i = 0, 1, \ldots, n$, the data of step 4 are measured and saved.

Step 6: Set $z_1 = -15 + i\delta_1$, $z_2 = -20 + (j-1)\delta_2 (j = 1, 2, \ldots, n+1)$, $\varphi = -20 + k\delta_3 (k = 1, 2, \ldots, n-1)$

Step 7: When $i = 0, 1, \ldots, n$, the data of step 6 are measured and saved.

Save all data to sj.txt file, and MATLAB program is edited as follows:

```
clear all
clc
importdata('e:\sj.txt');
x=ans(:,1);
y=ans(:,2);
z=ans(:,3);
[xx, yy]=meshgrid(-47:-25,-18:-22);
zz=griddata(x, y, z, xx, yy.'v4');
surf(xx, yy, zz);
shading interp;
```

These points are shown in a three-dimensional coordinate, then the workspace of the mechanism is obtained in Figure 9.

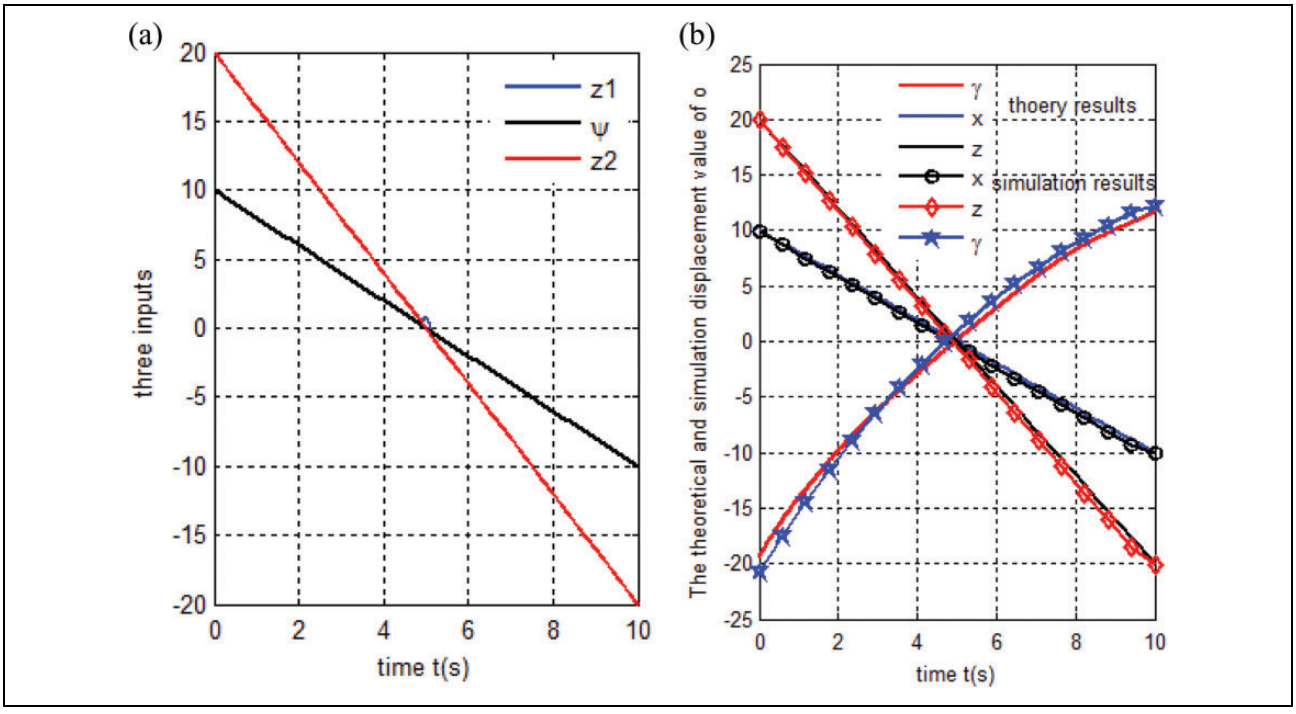


Figure 8. The kinematics simulation result. (a) Three initial inputs; (b) comparison of the theory and simulation value.

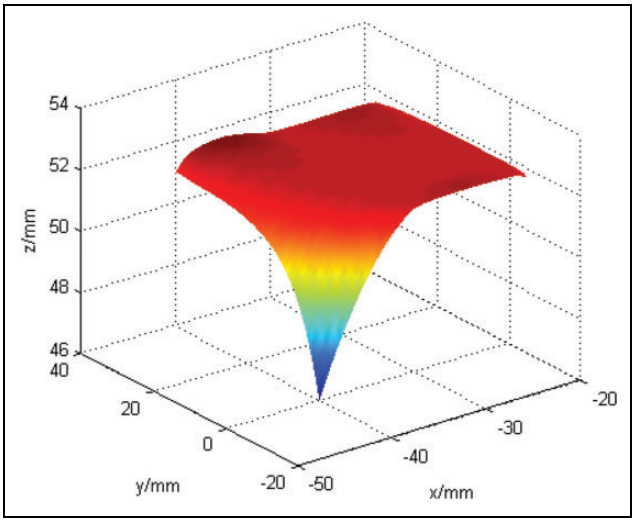


Figure 9. The workspace of 2PC-CPR parallel mechanism.

According to the workspace, the mechanism can be used to write Chinese characters such as "中" when a pen is installed at the center of moving platform. Besides, it can also be applied to productions classification, and so on.

Conclusion

In this article, a novel 2PC-CPR parallel mechanism is presented. The degree of freedom, kinematics analysis, dynamic model, SimMechanics model, and workspace of the parallel mechanism were investigated. We have come up with the following conclusions.

(1) The freedom degree of the parallel mechanism turns out to be three according to the screw theory, which proves that the parallel mechanism is reasonable. The input and output relationships of displacement, velocity, and acceleration are obtained by kinematics analysis. The Jacobian matrix is calculated out. The dynamic model is derived based on the virtual work principle, which presents the foundation for the control system.

(2) The kinematics SimMechanics model is established. Simulation results verify the theoretical derivations. The workspace of the parallel mechanism is analyzed based on kinematics SimMechanics model, and it can be imagined that our newly built mechanism has a promising future in the application of robot field.

Declaration of Conflicting Interests

The author(s) declared no potential conflicts of interest with respect to the research, authorship, and/or publication of this article.

Funding

The author(s) disclosed receipt of the following financial support for the research, authorship, and/or publication of this article: This work was financially supported in part by National Natural Science Foundation of China (no. 51105050).

Reference

1. Tsai LW, Walsh GC and Stamper RE. Kinematics of a novel three DOF translational platform. In *Collections of IEEE International Conference on Robotics and Automation*, Minneapolis, USA. 22–28 April 1996, pp. 3446–3451.
2. Han C and Kim J. Kinematic sensitivity analysis of the 3-UPU parallel mechanism. *J Mech Mach Theory* 2002; 37: 787–798.
3. Varedi SM, Daniali HM, and Ganji DD. Kinematics of an offset 3-UPU translational parallel manipulator by the homotopy continuation method. *Nonlinear Anal Real* 2009; 10: 1767–1774.
4. Ji P and Wu HT. Kinematics analysis of an offset 3-UPU translational parallel robotic manipulator. *J Robot Auto Syst* 2003; 42: 117–123.
5. Chebbi AH, Affi Z and Romdhane L. Prediction of the pose errors produced by joints clearance for a 3-UPU parallel robot. *J Mech Mach Theory* 2009; 44: 1768–1783.
6. Di Gregorio R and Parenti-Castelli V. Mobility analysis of the 3-UPU parallel mechanism assembled for a pure translational motion. *ASME J Mech Design* 2002; 124: 259–264.
7. Carricato M and Parenti-Castelli V. Singularity-free fully-isotropic translational parallel mechanisms. *Int J Robot Res* 2002; 21: 161–174.
8. Carricato M and Parenti-Castelli V. A series of 3-DOF translational parallel. *ASME J Mech Design* 2003; 125: 302–307.
9. Kong X and Gosselin CM. Kinematics and singularity analysis of a novel type of3-CRR 3-DOF translational parallel manipulator. *Int J Robot Res* 2002; 21: 791–798.
10. Li YM and Xu QS. Kinematic analysis and design of a new 3-DOF translational parallel manipulator. *ASME J Mech Design* 2006; 128: 729–737.
11. Ruggiu M. Kinematics analysis of the CUR translational manipulator. *J Mech Mach Theory* 2008; 43: 1087–1098.
12. Kim D and Chung WK. Kinematic condition analysis of 3-DOF pure translational parallel manipulators. *ASME J Mech Design* 2003; 125: 323–331.
13. Gosselin CM and Wang J. Singularity loci of a special class of spherical 3-DOF parallel mechanisms with revolute actuators. *Int J Robot Res* 2002; 21: 649–659.
14. Karouia M and Herve JM. A 3-DOF tripod for generating spherical rotation. In *Monograph of Advances in Robot Kinematics*, 2000, pp. 395–402.
15. Di Gregorio R. Statics and singularity loci of the 3-UPU wrist. *J IEEE Trans Robot* 2004; 20: 630–635.
16. Huang Z and Li QC. Construction and kinematic properties of 3-UPU parallel mechanisms. In *Proceedings of the ASME Design Engineering Technical Conference*, Montreal, Canada, 29 September–2 October 2002, pp. 1027–1033.
17. Lu Y and Hu B. Analysis of kinematics and solution of active/constrained forces of asymmetric 2UPU+X parallel manipulators. *J Mech Eng Sci* 2006; 220: 1819–1830.
18. Gong JL and Gao F (2006) *The robot mechanism configuration analysis based on movement and G_F set*. Ph.D. Thesis. Yanshan University, China, pp. 68–74.
19. Gong JL, Zhang YF and Gao F. The description method for the end of robot movement characteristics. *Mech Design* 2006; 23: 16–18.
20. Haas SL and Crossley FRE. A contribution to grubler's theory in the number synthesis of plane mechanisms. *Trans ASME J Eng Ind* 1969; 91B: 240–250.
21. Huang Z, Li QC and Ding HF. *Theory of parallel mechanisms*. Dordrecht: Springer, 2013.
22. Zhao YJ, Yang ZY and Huang T. Inverse dynamics of delta robot based on the principle of virtual work. *Trans Tianjin Univ* 2005; 11: 268–273.
23. Huang Z, Zhao YS and Zhao TS. *Advanced spatial mechanism*. Beijing: Higher Education Press 2006, Chapter 10.